



ALMA MATER STUDIORUM  
UNIVERSITÀ DI BOLOGNA

## ARCHIVIO ISTITUZIONALE DELLA RICERCA

### Alma Mater Studiorum Università di Bologna Archivio istituzionale della ricerca

Surface modification of nanocellulose through carbamate link for a selective release of chemotherapeutics

This is the final peer-reviewed author's accepted manuscript (postprint) of the following publication:

*Published Version:*

Surface modification of nanocellulose through carbamate link for a selective release of chemotherapeutics / Tortorella S.; Maturi M.; Dapporto F.; Spanu C.; Sambri L.; Comes Franchini M.; Chiariello M.; Locatelli E.. - In: CELLULOSE. - ISSN 0969-0239. - ELETTRONICO. - 27:(2020), pp. 8503-8511. [10.1007/s10570-020-03390-5]

*Availability:*

This version is available at: <https://hdl.handle.net/11585/788419> since: 2022-02-01

*Published:*

DOI: <http://doi.org/10.1007/s10570-020-03390-5>

*Terms of use:*

Some rights reserved. The terms and conditions for the reuse of this version of the manuscript are specified in the publishing policy. For all terms of use and more information see the publisher's website.

This item was downloaded from IRIS Università di Bologna (<https://cris.unibo.it/>).  
When citing, please refer to the published version.

(Article begins on next page)

This is the final peer-reviewed accepted manuscript of:

**Silvia Tortorella, Mirko Maturi, Francesca Dapporto, Chiara Spanu, Letizia Sambri, Mauro Comes Franchini, Mario Chiariello & Erica Locatelli “Surface modification of nanocellulose through carbamate link for a selective release of chemotherapeutics” *Cellulose*, 2020, 27(15), 8503-8511.**

The final published version is available online at: <https://dx.doi.org/10.1007/s10570-020-03390-5>

Terms of use:

Some rights reserved. The terms and conditions for the reuse of this version of the manuscript are specified in the publishing policy. For all terms of use and more information see the publisher's website.

*This item was downloaded from IRIS Università di Bologna (<https://cris.unibo.it/>)*

***When citing, please refer to the published version.***

# 1 **Surface Modification of Nanocellulose through** 2 **Carbamate Link for a Selective Release of** 3 **Chemotherapeutics**

4 Silvia Tortorella,<sup>a</sup> Mirko Maturi,<sup>a</sup> Francesca Dapporto,<sup>b</sup> Chiara Spanu,<sup>a</sup> Letizia  
5 Sambri,<sup>a</sup> Mauro Comes Franchini,<sup>a</sup> Mario Chiariello,<sup>b</sup> Erica Locatelli<sup>a\*</sup>

6

7 *(a) Department of Industrial Chemistry “Toso Montanari”, Viale Risorgimento 4,*  
8 *40136, Bologna, Italy.*

9 *(b) Consiglio Nazionale delle Ricerche (CNR), Istituto di Fisiologia Clinica (IFC),*  
10 *via Fioentina 1, 53100, Siena, Italy.*

11

12 Email: erica.locatelli2@unibo.it

13

14

## 15 **Abstract**

16 Herein we report the synthesis of cellulose nanocrystals covalently bound to a model  
17 chemotherapeutic drug (DOXO) via a novel spacer arm, which acts both as linker and as selective  
18 releasing agent. The carbamate linkage present in the linker, shows stability in aqueous  
19 environments for a wide range of conditions and can only be hydrolyzed in the presence of cells,  
20 freeing the active drug, with unmodified chemotherapeutics properties.

21

## 22 **Keywords**

23 Cellulose nanocrystals, carbamate linker, doxorubicin, selective release.

24

25

26

## 27 **Introduction**

28 Drug delivery is an important challenge in therapeutics. Setting up new formulations, technologies,  
29 and systems for properly achieving the delivery of pharmaceutical compounds is highly required

30 (Locatelli et al. 2014; Grünwald et al. 2016). In the past years, this field of research has increased in  
31 terms of studies and publications, mostly focused on polymer-based nanocarriers (Parhi et al. 2012;  
32 Sun et al. 2014).

33 Nanomaterials modification for the introduction of active agents onto their surface is the first  
34 requisite for creating an effective drug delivery system (Locatelli et al. 2015). Surface modification  
35 of nanomaterials with links and spacers has been the key for the introduction of active agents, such  
36 as proteins for targeted drug delivery, but it is also a powerful strategy to link on the drug' surface  
37 that should be selectively delivered: this is, nowadays, a topic in continuous development (Cellante  
38 et al. 2018).

39 Cellulose is the most abundant biopolymer in the world and, in its nanometric form, has wide  
40 potential as a component in bio nanocomposites. The use of nanocellulose in drug delivery systems  
41 is quite recent: until 2014 nanocellulose was mostly employed for reinforcing the structure of  
42 biomaterials (Dufresne 2013; Fatah et al. 2014; Gazzotti et al. 2019; Peres et al. 2019). After 2014,  
43 advancements on its chemical processing have strongly pushed the research in biomedical  
44 engineering, also due to the low cost of the starting material and the tunable properties of the final  
45 nanosystems (Habibi 2014; Khine et al. 2020).

46 One potential and partially explored application of nanocellulose may be in cancer therapy, as  
47 nanocarrier for drug transport and release, since its sugar-based backbone allows for easy chemical  
48 modification and for a total biocompatibility, absence of cyto- and systemic toxicity, and easy  
49 excretion via cell digestion (Lin and Dufresne 2014). Anyways, there are still many issues to be  
50 addressed: indeed, the main challenge remains the development of strategies for a controlled surface  
51 modification in order to link or incorporate a drug in a stable and reproducible way and, most  
52 important, to have a long and controlled release over time.

53 Dash et al. in 2012 worked on cellulose nanocrystals (CNCs) for a new 'alternative' drug delivery  
54 system: with the help of aromatic linkers and spacer molecules, they tried the attachment of active  
55 amine-containing drugs to the CNCs (Dash and Ragauskas 2012). However, only the introduction  
56 of a spacer arm was completed, but neither the creation of a cleavable linker nor the incorporation  
57 of the drug was attempted.

58 Carbamates, the esters of carbamic acid, are well known in organic chemistry, especially for their  
59 presence in amine-protecting group such as tert-butyloxycarbonyl (Boc), fluorenylmethoxycarbonyl  
60 (Fmoc) and carboxybenzyl (Cbz). Due to their hydrolytic stability, carbamates have been used in  
61 the design of prodrugs in order to achieve prolonged systemic circulation (Ghosh and Brindisi 2015).  
62 Conversion of carbamate prodrugs in body requires the presence of specific enzymes (e.g. esterase)  
63 for the release of the parent drug. Upon hydrolysis, carbamate esters release the corresponding  
64 alcohol and carbamic acid, which, due to its chemical instability, immediately breaks down to the  
65 corresponding amine, thus releasing the free drug and carbon dioxide.

66 Achieving the release of payloads at the target sites in a spatial- and/or time-controlled manner has  
67 been reviewed as the real peculiarity of advanced controlled drug delivery systems (DDSs), which  
68 can effectively reduce the dosage frequency, while maintaining the drug concentration in targeted  
69 organs/tissues for a longer period of time. This became of the utmost importance when applying  
70 therapeutics with high toxicological side effects, such as chemotherapeutics. The local, prolonged  
71 and smart release of drugs is the only possibility in future for personalized sustained and sustainable  
72 therapies, and the research of novel carriers, such the one proposed in this paper, is of tremendous  
73 demanding (Liu et al. 2016).

74 Inspired by these medical needs and by the above mentioned data, in this paper we report the linkage  
75 of an amino-containing model drug (Doxorubicin, DOXO) onto CNCs via the surface modification  
76 of the nanosystem and the creation of a linker that can be easily shortcut by cellular enzymes, finally  
77 releasing the active molecules unaltered. Several release conditions were investigated finding an  
78 extreme stability of the linkers. Indeed, the release can only happen by an enzyme-cleaved initiation  
79 step to separate the linker from the drug and, through decomposition of the linkers, to deliver the  
80 unmodified drug (Casey Laizure et al. 2013). With our strategy the drug appears fully active after  
81 the release and its efficacy has been proved *in vitro* by cells death assessing.

82

83

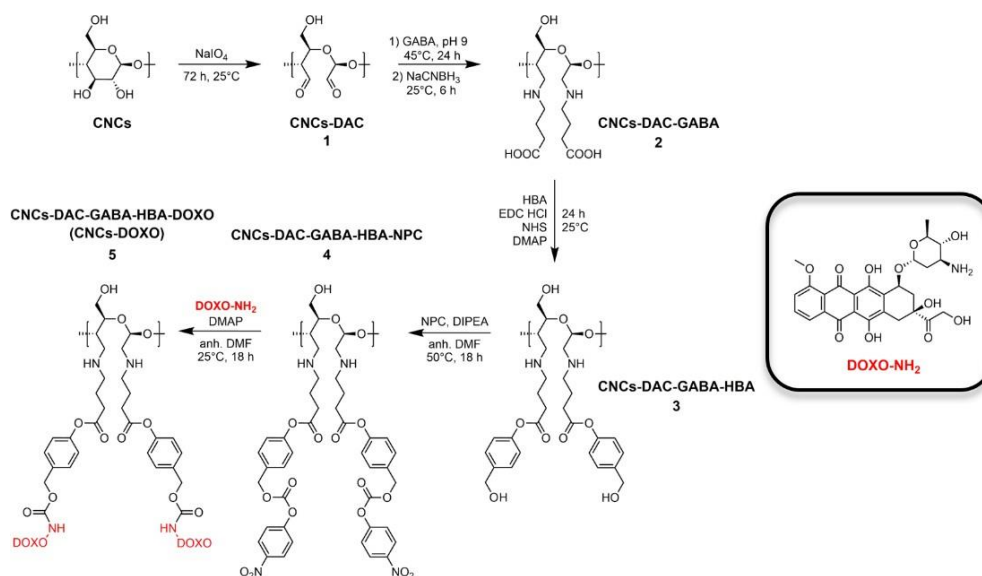
84

## 85 **Results and Discussion**

### 86 **Synthesis and Chemical Modification**

87 The nanocarrier was synthesized using pure cellulose filter paper as starting material. This has been  
88 digested in acidic environment to produce cellulose nanocrystals, which have been chemically  
89 modified on their surface to stably bind the active drug via a series of 5 consecutive reactions (**Fig.**  
90 **1**).

91



92

93 **Fig. 1.** Schematic representation of the synthetic step for the preparation of Doxorubicin-loaded  
 94 CNCs. Abbreviations: CNCs = cellulose nanocrystals, DAC = cellulose dialdehyde, GABA =  $\gamma$ -  
 95 amino butyric acid, HBA = 4-hydroxy benzyl alcohol, EDC HCl = 1-ethyl-3-(3-  
 96 dimethylaminopropyl)carbodiimide hydrochloride, NHS = N-hydroxy succinimide, DMAP = 4-  
 97 dimethylamino pyridine, NPC = 4-nitrophenyl chloroformate, DIPEA = N,N-diisopropyl-N-  
 98 ethylamine, anh. DMF = anhydrous dimethylformamide, DOXO-NH<sub>2</sub> = doxorubicin  
 99

100 Cellulose nanocrystals (CNCs) were prepared according to a reported procedure, with slight  
 101 modifications (Jiang et al. 2010). The DLS (Dynamic Light Scattering) analysis of hydrolyzed CNCs  
 102 revealed a  $\zeta$ -potential value of -11.0 mV as expected for fully hydroxylated sugars-based structures  
 103 (Mahouche-Chergui et al. 2014). The IR spectrum is reported in **Fig. 2a**.

104 The so-obtained CNCs have been then treated with the strong oxidizing agent NaIO<sub>4</sub>, so as to lead  
 105 to the opening of the sugar ring with selective rupture of the  $\sigma$  C<sub>2</sub>-C<sub>3</sub> bond and to the introduction of  
 106 two aldehydic residues. The resulting product, dialdehyde cellulose (CNCs-DAC, 1), showed an  
 107 unmodified  $\zeta$ -potential value of -11.2 mV, in accordance with the introduction of non-charged  
 108 functional groups. The IR analysis (**Fig. 2b**) revealed the presence of a signal (even if with poor  
 109 intensity) at 1734 cm<sup>-1</sup> that can be attributed to the C=O of the aldehydes. The low intensity of the  
 110 carbonyl stretching absorption can be related to the equilibrium that exist in water between  
 111 aldehydes and geminal diols, catalyzed by both acidic and alkaline conditions, and by the occurrence  
 112 of intramolecular hemiacetals (Buschmann et al. 1982). Moreover, the aldehyde content of  
 113 periodate-oxidized CNCs was determined to be as high as 0.15 mmol of aldehydes per gram of  
 114 CNCs-DAC, revealing extensive oxidation of CNCs surface.

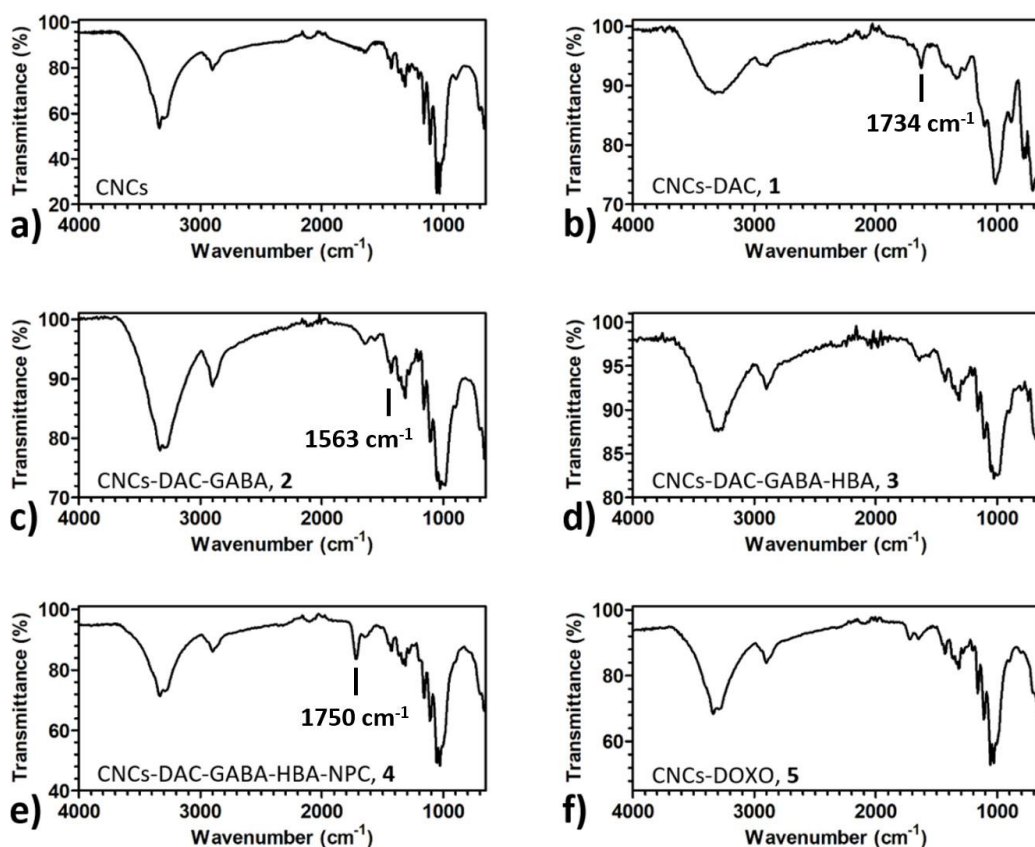
115 CNCs-DAC has been then coupled with  $\gamma$ -aminobutyric acid (GABA) through a reductive amination  
 116 in presence of the reducing agent sodium cyanoborohydride (NaCNBH<sub>3</sub>): in this reaction, each of  
 117 the CNCs aldehyde groups react with the amino group presents in the GABA, thus forming an imine

118 (Schiff base), which is then reduced in the second step, linking the GABA residues to the cellulose  
119 backbone through stable amino groups. The obtained product (CNCs-DAC-GABA, **2**) is then  
120 purified and characterized: the  $\zeta$ -potential value has been found equal to - 31.6 mV, which agrees  
121 with the introduction of carboxylic groups that are generally deprotonated at neutral pH and able to  
122 confer a high negative surface charge. The FTIR analysis (**Fig. 2c**) showed the disappearance of the  
123 signal attributed to the aldehyde groups at  $1734\text{ cm}^{-1}$  and the appearance of a new signal at  $1563\text{ cm}^{-1}$   
124 related to the stretching of N-H bonds.

125 At this point, the nucleophilic substitution with the aromatic linker 4-hydroxybenzyl alcohol (HBA)  
126 has been carried out in presence of the coupling agent 1-ethyl-3-(3-dimethylamino propyl)  
127 carbodiimide hydrochloride (EDC-HCl) that allows the esterification reaction to proceed in water.  
128 The obtained CNCs-DAC-GABA-HBA, **3** presents a  $\zeta$ -potential value of -15.2 mV, in agreement  
129 with the disappearance of -COOH groups in favor of less charged hydroxyl groups. The FTIR  
130 analysis (**Fig. 2d**) showed little or no variation in comparison to the previous one.

131 Dash and Ragauskas described the synthesis until this step, but nothing more was attempted for the  
132 actual linkage of a drug to CNCs (Dash and Ragauskas 2012). In order to proceed with the  
133 functionalization of CNCs and the creation of a cleavable linker, an acylation reaction with 4-  
134 nitrophenylchloroformate was performed in anhydrous DMF. The product (CNCs-DAC-GABA-  
135 HBA-NPC, **4**) presents now a carbonate group, suitable for nucleophilic substitution with amino  
136 groups. Since this functional group tends to hydrolyze in aqueous environments, the HBA-linked  
137 CNCs has been preventively freeze-dried so as to remove most of the water before dissolution in  
138 DMF.  $\zeta$ -potential analysis was not performed because of this inconvenience. Anyways, the FTIR  
139 analysis (**Fig. 2e**) showed an intense signal appearing at  $1750\text{ cm}^{-1}$  due to the carbonate group, thus  
140 confirming the reaction's success.

141 Finally, an amino containing drug could be loaded to CNCs by nucleophilic substitution on the  
142 carbonate group on the linker (**Fig. 2f**). As a model drug, Doxorubicin was selected since it contains  
143 a single amino group able to react with the linker, and it produces a strong fluorescence that allows  
144 for its easy determination and quantification. The selected solvent for the coupling reaction remains  
145 anhydrous DMF, but the final product (CNCs-DAC-GABA-HBA-DOXO or CNCs-DOXO, **5**) can  
146 be re-dispersed in water after purification, due to the creation of water-stable carbamide bonds. A  
147 strong red coloration easily indicates that the reaction proceeds in the desired way and that  
148 Doxorubicin has been linked to CNCs. Fluorometric analysis revealed a Doxorubicin loading equal  
149 to 0.25% w/w, which is a satisfactory result since only the surface of CNCs can be exploited for  
150 functionalization, while the entire core of the nanosystem remains unaffected by the reactions.



151151

152 **Fig. 2.** ATR-FTIR analysis of the modified cellulose products. CNCs (a); CNCs-DAC, **1** (b); CNCs-  
 153 DAC-GABA, **2** (c); CNCs-DAC-GABA, **3** (d); CNCs-DAC-GABA-NPC, **4** (e) and CNCs-DOXO,  
 154 **5** (f)

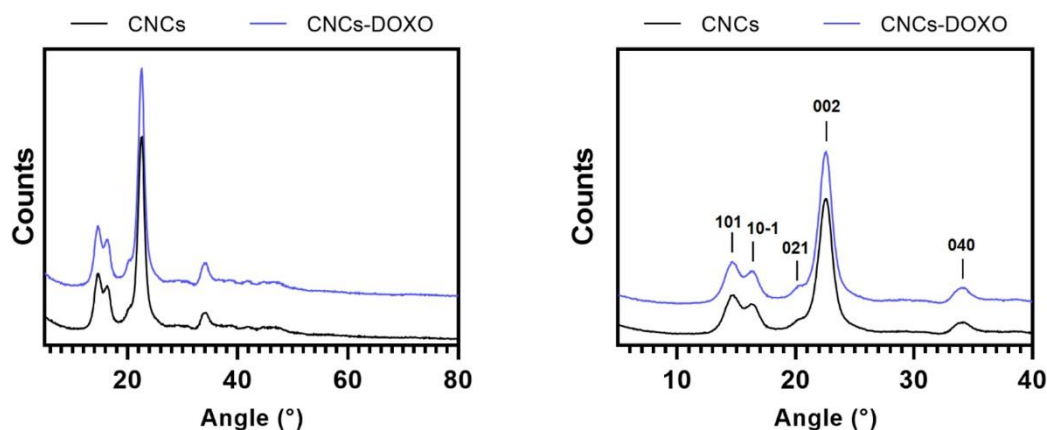
155

156 The mechanism of drug release by this carbamate linker was also discussed by Dash et al., who  
 157 theorized the possible drug release via 1-6 elimination of the 4-hydroxy benzyl alcohol. This would  
 158 lead to the release of DOXO-NH-CO-O-CH<sub>2</sub>PhOH rather than DOXO-NH<sub>2</sub>, with unknown effects  
 159 on the drug efficacy. In order to demonstrate the efficient release of the pristine drug, we  
 160 analyzed by <sup>1</sup>H-NMR the chemical nature of the released species at different pH  
 161 (**Supplementary Fig. 2**). At pH 12, DOXO-NH<sub>2</sub> was released without the presence of any sign  
 162 of 1-6 elimination of the 4-hydroxy benzyl alcohol, therefore demonstrating the integrity of the  
 163 released drug by cleavage of the carbamate bond.

164 The crystallinity of CNCs was confirmed to be unchanged during the conjugation steps by applying  
 165 XRD on freeze-dried CNCs-DOXO compared to pristine CNCs (**Fig. 3** and **Supplementary Table**  
 166 **2**). This analysis revealed no variation in the crystallinity of CNCs after the formation of the DOXO  
 167 linkage.

168168





169169

170 **Fig. 3.** XRD analysis (Cu K $\alpha$ ) on freeze-died CNCs compared to CNCs-DOXO. Full spectrum  
 171 (left) and its expansion with the *hkl* assignment of the peaks (right).

172172

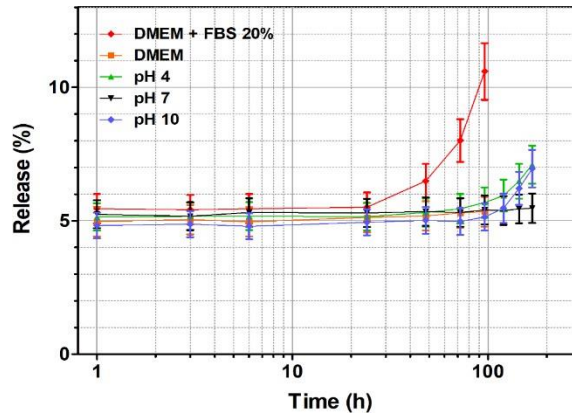
173173

174174

## 175 Release studies

176 In order to investigate the stability of the carbamate linker and the conditions required to achieve  
 177 drug release in vitro, several tests have been performed. In particular, CNCs-DOXO was incubated  
 178 at 37°C in D.I. water (pH 6.5), in alkaline (pH 10) and acid (pH 4.5) environments, in DMEM and  
 179 finally in DMEM containing 20% of fetal bovine serum (FBS). Drug release was followed over 96  
 180 h or 1 week when possible and compared to the total amount of doxorubicin loaded onto CNCs (**Fig.**  
 181 **4**). A burst release of drug (around 5.5% of the total) was observed within the first hour  
 182 independently on the release medium: this could be related to the release of physisorbed Doxorubicin  
 183 from CNCs, not related to the cleavage of any covalent linking. Interestingly, little drug release was  
 184 observed only in the presence of FBS after at least 24 h, revealing the great stability of the proposed  
 185 linker in aqueous environment. We believe enzymes and/or proteins in FBS are able to partially  
 186 trigger the release of DOXO, with an empirical kinetics by which the amount of released drug is  
 187 proportional to squared time (**Supplementary Fig. 3 and 4**). As expected, after 96 h DMEM  
 188 medium starts to degrade: this is a peculiar property of this agent which helps biologists to monitor  
 189 cell growth and maintenance, but does not allow us to prolong the corresponding release study  
 190 longer.

191191

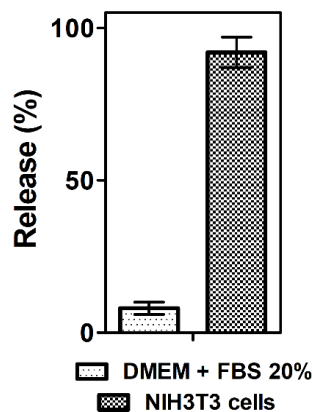


192192

193 **Fig. 4.** Release kinetics of Doxorubicin from CNCs-DOXO in different solutions at 37°C,  
 194 determined by fluorometric analysis. Release is observed in DMEM + FBS 20%.

195195

196 Since the drug binding to the nanocarrier demonstrated its stability in normal conditions, we tested  
 197 whether the release of DOXO could be triggered by cells themselves, which contain a much greater  
 198 variety of enzymes (such as carboxylesterases) that could cleave the carbamate linker. In order to  
 199 explore that, CNCs-DOXO has been dispersed in cell culture media containing NIH3T3 cells. After  
 200 96 h of incubation at 37°C, a portion of the medium is withdrawn and centrifugated to remove  
 201 nanostructures and cells. Fluorescence analysis on the obtained supernatant revealed that around  
 202 94% of the CNCs-loaded DOXO was released as free drug, revealing that the complete release of  
 203 DOXO can only be achieved by the direct action of cells, while the drug remains stably connected  
 204 to cellulose in non-biological systems (**Fig. 5**).



205205

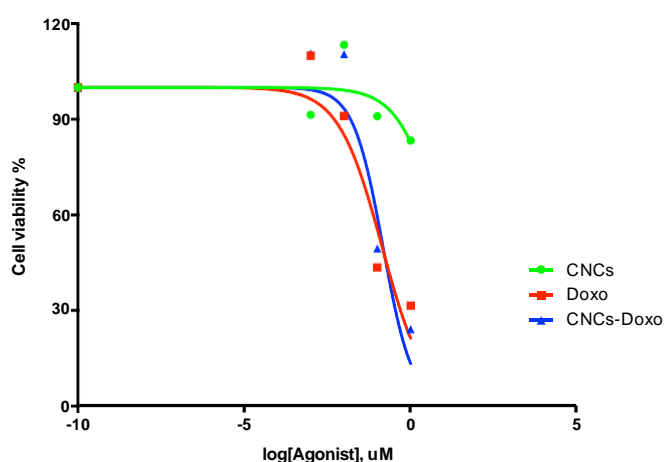
206 **Fig. 5:** Comparison between the released amount of Doxorubicin after 72 h of incubation at 37°C  
 207 either in DMEM + FBS 20% or in NIH3T3 cell culture.

208208

## 209 In vitro studies – Cell Viability Assay

210 The cytotoxicity of CNCs-DOXO was evaluated in NIH3T3 cells by a MTS cell viability assay.  
211 Specifically, NIH3T3 cells were treated with increasing concentrations of CNCs-DOXO and  
212 compared to equivalent amounts of bare CNCs and free DOXO (**Fig. 6**). Interestingly, the obtained  
213  $IC_{50}$  values showed almost identical effects of free doxorubicin ( $IC_{50} = 1.139 \mu M$ ) and CNCs-DOXO  
214 ( $IC_{50} = 1.148 \mu M$ ), confirming that cells are able to cut the carbamate linker between CNCs and  
215 DOXO, thereby releasing the drug for its cytotoxic action. Importantly, bare CNCs showed very  
216 little toxicity at concentrations required for carrying sufficient concentrations of active DOXO ( $IC_{50}$   
217  $= 9.505 \mu M$ ).

218



219

220

221 **Fig. 6.** Cell viability assay in NIH3T3 cells. MTS assay was performed after 72 h treatment of  
222 NIH3T3 cells with different concentrations of CNCs, DOXO and CNCs-DOXO, to establish relative  
223  $IC_{50}$  values. The results shown are averages of triplicate samples from a typical experiment.

224

225

## 226 Conclusions

227 In conclusion, we have reported for the first time an effective linker based on carbamate cleavable  
228 group for the attachment of model drug (Doxorubicin) to nanocellulose crystal backbone. The  
229 protocol for linking the drug is reproducible and easy to handle. The linker, consisting of a spacer  
230 arm and the carbamate prodrug, has been proved to be stable under harsh conditions, such as basic  
231 or acidic pH. On the other hand, the release of the active and unaltered drug is achieved in almost  
232 quantitative way in presence of cells owning proper enzymes for carbamate cleavage.

233 To the best of our knowledge this surface modification of CNCs represents the first successful  
234 obtainment of a cleavable linker for incorporation of drugs, thus allowing for the very first time the

235 usage of nanocellulose as proper smart drug delivery system. This modern approach represents the  
236 first step towards the use of completely bio-based nanomaterials able to ensure more stimulus-  
237 sensitive and sustained nanomedicine for clinical applications.  
238238

## 239 **Experimental section**

240 All chemicals have been purchased from Sigma-Aldrich Co. (St Louis, MO, USA) and used as  
241 received. Amount of DOXO linked to the nanocarrier was determined by fluorescence analysis with  
242 an Edimburg FLSP920 spectrofluorimeter equipped with a 450 W Xenon arc lamp. All aqueous  
243 solutions were prepared with deionized water obtained using an ultrafiltration system (Milli-Q;  
244 EMD Millipore, Billerica, MA, USA) with a measured resistivity above 18 MΩ/cm. XRD analysis  
245 has been performed with a vertical goniometric diffractometer (Bragg – Brentano geometry) Philips  
246 PW 1050/81 with a PW 1710 chain counting employing Cu K $\alpha$  radiation. **<sup>1</sup>H-NMR spectra were  
247 obtained on a Varian Inova (14.09 T, 600 MHz) NMR spectrometer. In all recorded spectra,  
248 chemical shifts have been reported in ppm of frequency relative to the residual solvent signals for  
249 both nuclei (<sup>1</sup>H: 4.79 ppm for D<sub>2</sub>O). Solvent-suppressed <sup>1</sup>H-NMR spectra have been recorded with  
250 pre-saturation pulse sequences.**

251251

## 252 **Synthesis of CNCs**

253 1.5 g of Whatman® cellulose filter paper is finely cut and placed in a 250 mL round-bottomed flask.  
254 At this point, 25 mL of ice-cold 4 M aqueous HCl solution are added under stirring. After all the  
255 filter paper was soaked in the acid solution, the flask is moved to an oil bath set at 80°C under  
256 continuous stirring for 4 h. Hydrolysis is stopped by addition of 70 mL of cold water. Then, the  
257 milky suspension is summarily purified by centrifugation (6000 rpm, 15 min) and redispersion in  
258 water, and finally by dialysis. Reaction yield (68%) was determined by gravimetric analysis of the  
259 final aqueous dispersion, and CNCs was stored in the fridge at a concentration of 2%.

260260

## 261 **Synthesis of CNCs-DAC, 1:**

262 In a 100 mL flask, 15 mL of the 2% CNCs dispersion are added to 155 mg of NaIO<sub>4</sub>. The flask is  
263 then wrapped in aluminium foil to protect it from the light, and the reaction is allowed to take place  
264 for 72 h by stirring at room temperature. Then, the synthesized CNCs-DAC is separated by  
265 centrifugation, dispersed in water and dialyzed. The final concentration of DAC was again 2%. The  
266 total aldehyde content was determined exploiting the fluorimetric method reported by Nonsuwan in

267 2009, in which aldehydes are reacted with acetoacetanilide and ammonium acetate exploiting  
268 Hantzsch's reaction to quantitatively produce a fluorophore. (Nonsuwan et al. 2019).

269269

### 270 **Synthesis of CNCs-DAC-GABA, 2:**

271 10 mL of 2% CNCs-DAC are added to 10 mL of 0.2 M sodium acetate solution (pH 9) in a 50 mL  
272 round-bottomed flask, and stirred for 15 min. Then, 1.143 g of  $\gamma$ -aminobutyric acid (GABA) are  
273 added. Reaction is carried out by stirring at 45°C for 24 h. After cooling, 175 mg of NaCNBH<sub>3</sub> are  
274 added, and the mixture is further stirred for 6 h. Reaction mixture is purified by dialysis and  
275 centrifugation. Gravimetric analysis on the purified product reveals a 32% yield and a concentration  
276 of the final solution equal to 0.63% w/w.

277277

### 278 **Synthesis of CNCs-DAC-GABA-HBA, 3:**

279 From the previous step, 10 mL of a 0.63% dispersion of 2 are transferred to a 50 mL flask, to which  
280 576 mg of EDC HCl, 33 mg of NHS, 384 mg of DMAP and 337 mg of HBA are sequentially added.  
281 The mixture is magnetically stirred for 24 h at room temperature, then purified by dialysis and  
282 freeze-dried. Final yield was 79%.

283283

### 284 **Synthesis of CNCs-DAC-GABA-HBA-NPC, 4:**

285 In a dry 50 mL flask and under N<sub>2</sub> atmosphere, 78.2 mg of 3 are dispersed in 20 mL of anhydrous  
286 DMF. Then, 715 mg of 4-nitrophenyl chloroformate (NPC) and 50  $\mu$ L of DIPEA are added. The  
287 mixture is placed in an oil bath set at 50°C and stirred for 18 h, after which the mixture was washed  
288 by addition of 5 mL of water and successive centrifugation. Then, in order to remove most of the  
289 water, the precipitated pellet is dispersed in anhydrous DMF and centrifugated several times, each  
290 time discarding the hydrate DMF supernatant. Finally, the pellet was dispersed in 5 mL of anhydrous  
291 DMF to proceed with the conjugation of the drug.

292292

### 293 **Linkage of Doxorubicin: synthesis of CNCs-DAC-GABA-HBA-DOXO,** 294 **5:**

295 The entire amount of product obtained by the previous step is added to 121 mg of DMAP dissolved  
296 in 5 mL of anhydrous DMF, in a round-bottomed flask under N<sub>2</sub> flow. Then, 1 mL of 1 mg mL<sup>-1</sup>

297 doxorubicin solution is added. Coupling reaction is allowed to happen by stirring at room  
298 temperature for 18 h, after which the unbound excess of doxorubicin was eliminated by repeated  
299 centrifugation and washes with water, until clear supernatant and red pellet were obtained. The  
300 suspension is then freeze-dried and stored at room temperature under vacuum.  
301301

## 302 Quantification of Doxorubicin

303 The amount of doxorubicin (DOXO) in all solutions was determined by fluorometric analysis. Four  
304 standard CNCs aqueous solutions at 0.1, 0.2, 0.4 and 0.8  $\mu\text{g mL}^{-1}$  are prepared and their fluorescence  
305 emission intensity was detected at 594 nm while exciting at 288 nm. Linear correlation was observed  
306 between the counts at the detector and the concentrations, allowing to use fluorescence intensity to  
307 measure DOXO concentration, maintaining constant all other experimental parameters  
308 (Supplementary Fig. 1).  
309309

## 310 NMR analysis of the released species

311 In order to establish the chemical nature of the released species at different pH, 15 mg of freeze-  
312 dried CNCs-DOXO have been dispersed in 1.5 mL of D<sub>2</sub>O and divided in three 500  $\mu\text{L}$  portions that  
313 are added to 500  $\mu\text{L}$  of 2 M, 0.02 M and 0.0002 M NaOH in H<sub>2</sub>O, respectively, to achieve pH values  
314 of 10, 12 and 14. At pH 12 the solution turned purple to the deprotonation of DOXO and blue at pH  
315 14 due to DOXO decomposition. After overnight incubation at room temperature, samples have  
316 been acidified with aqueous HCl and the dispersions have been microfiltered using 440 nm pore-  
317 size syringe filters and underwent <sup>1</sup>H-NMR analysis with solvent suppression pulse sequence.  
318318

## 319 Release Studies

320 Release studies were performed by placing 800  $\mu\text{L}$  of a 25  $\text{mg mL}^{-1}$  dispersion of CNCs-DOXO  
321 inside a Slide-A-Lyzed MINI dialysis device equipped with a membrane with MWCO of 2 kDa and  
322 placed into 10 mL of the release medium at 37°C. At predetermined time steps, 2 mL of the release  
323 medium are withdrawn to undergo free DOXO quantification by fluorescence analysis and replaced  
324 with 2 mL of pure water at 37°C. Buffer at pH 7 was prepared using NaH<sub>2</sub>PO<sub>4</sub>/Na<sub>2</sub>HPO<sub>4</sub> 0.1 M,  
325 buffer at pH 4 using CH<sub>3</sub>COOH/CH<sub>3</sub>COONa 0.1 M and at pH 10 using NaHCO<sub>3</sub>/Na<sub>2</sub>CO<sub>3</sub> 0.1 M.  
326326

## 327 **In vitro studies – Cell Viability Assay**

328 The antiproliferative effect of CNCs, DOXO and CNCs-DOXO in NIH3T3 cells was measured  
329 using the CellTiter 96 AQueous One Solution Cell Proliferation Assay Kit (Promega, Madison, WI,  
330 USA), following the manufacturer’s protocol. Briefly, approximately  $1 \times 10^3$  cells were seeded into  
331 each well of a flat-bottom 96-well cell culture plate in 100  $\mu\text{L}$  of recommended culture medium and  
332 were allowed to grow for 24 h at 37°C with 5%  $\text{CO}_2$ . After 24 h of incubation, culture medium was  
333 replaced by fresh medium containing the different test agents. The concentrations of CNCs, DOXO  
334 and CNCs-DOXO were gradually increased from 0 to 10  $\mu\text{M}$  (0.000, 0.001, 0.010, 0.100, 1.000,  
335 10.000  $\mu\text{M}$ ). Seeded 96-well plates were then incubated for 72 h at 37°C with 5%  $\text{CO}_2$ . 20  $\mu\text{L}$  of  
336 CellTiter 96 AQueous One Solution Cell Proliferation Assay reagent were then added for 2 h at 37  
337 °C. The signal was detected using VersaMax MicroPlate Reader (Molecular Device, San Jose, CA  
338 USA). The relative growth (compared with the cell viability at 0 h) of the cells was then calculated  
339 using the equation:  $[A]_T/[A]_{T_0}$ , where  $[A]_T$  is the absorbance at time point T and  $[A]_{T_0}$  is the  
340 absorbance at 0 h. The assay was performed in triplicate.

341

342

## 343 **References**

- 344 Buschmann H-J, Dutkiewicz E, Knoche W (1982) The Reversible Hydration of Carbonyl  
345 Compounds in Aqueous Solution Part II: The Kinetics of the Keto/Gem-diol Transition.  
346 *Berichte der Bunsengesellschaft für Phys Chemie* 86:129–134.  
347 <https://doi.org/10.1002/bbpc.19820860208>
- 348 Casey Laizure S, Herring V, Hu Z, et al (2013) The Role of Human Carboxylesterases in Drug  
349 Metabolism: Have We Overlooked Their Importance? *Pharmacother J Hum Pharmacol Drug*  
350 *Ther* 33:210–222. <https://doi.org/10.1002/phar.1194>
- 351 Cellante L, Costa R, Monaco I, et al (2018) One-step esterification of nanocellulose in a Brønsted  
352 acid ionic liquid for delivery to glioblastoma cancer cells. *New J Chem* 42:5237–5242.  
353 <https://doi.org/10.1039/C7NJ04633B>
- 354 Dash R, Ragauskas AJ (2012) Synthesis of a novel cellulose nanowhisker-based drug delivery  
355 system. *RSC Adv* 2:3403–3409. <https://doi.org/10.1039/c2ra01071b>
- 356 Dufresne A (2013) Nanocellulose: a new ageless bionanomaterial. *Mater Today* 16:220–227.  
357 <https://doi.org/10.1016/j.mattod.2013.06.004>
- 358 Fatah I, Khalil H, Hossain M, et al (2014) Exploration of a Chemo-Mechanical Technique for the  
359 Isolation of Nanofibrillated Cellulosic Fiber from Oil Palm Empty Fruit Bunch as a  
360 Reinforcing Agent in Composites Materials. *Polymers (Basel)* 6:2611–2624.  
361 <https://doi.org/10.3390/polym6102611>

- 362 Gazzotti S, Rampazzo R, Hakkarainen M, et al (2019) Cellulose nanofibrils as reinforcing agents  
363 for PLA-based nanocomposites: An in situ approach. *Compos Sci Technol* 171:94–102.  
364 <https://doi.org/10.1016/j.compscitech.2018.12.015>
- 365 Ghosh AK, Brindisi M (2015) Organic Carbamates in Drug Design and Medicinal Chemistry. *J*  
366 *Med Chem* 58:2895–2940. <https://doi.org/10.1021/jm501371s>
- 367 Grünwald B, Vandooren J, Locatelli E, et al (2016) Matrix metalloproteinase-9 (MMP-9) as an  
368 activator of nanosystems for targeted drug delivery in pancreatic cancer. *J Control Release*  
369 239:39–48. <https://doi.org/10.1016/j.jconrel.2016.08.016>
- 370 Habibi Y (2014) Key advances in the chemical modification of nanocelluloses. *Chem Soc Rev*  
371 43:1519–1542. <https://doi.org/10.1039/C3CS60204D>
- 372 Jiang F, Esker AR, Roman M (2010) Acid-Catalyzed and Solvolytic Desulfation of H<sub>2</sub>SO<sub>4</sub> -  
373 Hydrolyzed Cellulose Nanocrystals. *Langmuir* 26:17919–17925.  
374 <https://doi.org/10.1021/la1028405>
- 375 Khine YY, Batchelor R, Raveendran R, Stenzel MH (2020) Photo-Induced Modification of  
376 Nanocellulose: The Design of Self-Fluorescent Drug Carriers. *Macromol Rapid Commun*  
377 41:1900499. <https://doi.org/10.1002/marc.201900499>
- 378 Lin N, Dufresne A (2014) Nanocellulose in biomedicine: Current status and future prospect. *Eur*  
379 *Polym J* 59:302–325. <https://doi.org/10.1016/j.eurpolymj.2014.07.025>
- 380 Liu D, Yang F, Xiong F, Gu N (2016) The Smart Drug Delivery System and Its Clinical Potential.  
381 *Theranostics* 6:1306–1323. <https://doi.org/10.7150/thno.14858>
- 382 Locatelli E, Monaco I, Comes Franchini M (2015) Surface modifications of gold nanorods for  
383 applications in nanomedicine. *RSC Adv* 5:21681–21699.  
384 <https://doi.org/10.1039/C4RA16473C>
- 385 Locatelli E, Naddaka M, Uboldi C, et al (2014) Targeted delivery of silver nanoparticles and  
386 alisertib: in vitro and in vivo synergistic effect against glioblastoma. *Nanomedicine* 9:839–  
387 849. <https://doi.org/10.2217/nnm.14.1>
- 388 Mahouche-Chergui S, Grohens Y, Balnois E, et al (2014) Adhesion of Silica Particles on Thin  
389 Polymer Films Model of Flax Cell Wall. *Mater Sci Appl* 05:953–965.  
390 <https://doi.org/10.4236/msa.2014.513097>
- 391 Nonsuwan P, Matsugami A, Hayashi F, et al (2019) Controlling the degradation of an oxidized  
392 dextran-based hydrogel independent of the mechanical properties. *Carbohydr Polym*  
393 204:131–141. <https://doi.org/10.1016/j.carbpol.2018.09.081>
- 394 Parhi P, Mohanty C, Sahoo SK (2012) Nanotechnology-based combinational drug delivery: an  
395 emerging approach for cancer therapy. *Drug Discov Today* 17:1044–1052.  
396 <https://doi.org/10.1016/j.drudis.2012.05.010>
- 397 Peres BU, Vidotti HA, de Carvalho LD, et al (2019) Nanocrystalline cellulose as a reinforcing  
398 agent for electrospun polyacrylonitrile (PAN) nanofibers. *J Oral Biosci* 61:37–42.



399 <https://doi.org/10.1016/j.job.2018.09.002>  
400 Sun T, Zhang YS, Pang B, et al (2014) Engineered Nanoparticles for Drug Delivery in Cancer  
401 Therapy. *Angew Chemie Int Ed* 53:n/a-n/a. <https://doi.org/10.1002/anie.201403036>  
402